Applied Physics Letters ARTICLE pubs.aip.org/aip/apl

Capacitance–voltage extraction method for the deep-level defect distribution in organic photodiode

Cite as: Appl. Phys. Lett. **123**, 263504 (2023); doi: 10.1063/5.0179058
Submitted: 29 September 2023 · Accepted: 8 December 2023 ·
Published Online: 26 December 2023

Wencai Zuo, Sai Liu, Haoyang Li, Lianjie Zhang,[a] Weijing Wu,[a] Junwu Chen, and Junbiao Peng

AFFILIATIONS

Institute of Polymer Optoelectronic Materials and Devices, State Key Laboratory of Luminescent Materials and Devices, South China University of Technology, Guangzhou 510640, China

[a]Authors to whom correspondence should be addressed: lianjiezhang@scut.edu.cn and wuwj@scut.edu.cn

ABSTRACT

This paper proposes a method to extract deep-level trap states of the organic photodiode by capacitance–voltage (CV) measurement. The relationship between the trapped charge density and the surface potential can be determined by solving Poisson's equation, while employing Gauss's theorem to establish a correlation between the charge density and the CV characteristics. Consequently, deep-level trap states can be analytically obtained by the conventional CV measurement. Experimental results on P3HT:PCBM devices demonstrate that the deep trap distribution obtained by this method can be well connected with the capacitance–frequency method. Furthermore, our CV method yields a total trap concentration, which closely aligns with that obtained through Mott–Schottky relation. In conclusion, this method provides an effective approach for quantifying deep trap state density of organic photodiode.

Organic semiconductor materials have wide applications in solar cells,[1,2] photodetector,[3,4] light emitting diodes,[5,6] and field-effect transistors.[7] Compared with the crystal structure of inorganic materials, organic semiconductor materials tend to show more defects due to their disorder.[1] Trap states within the energy gap have a significant impact on carrier transport in organic semiconductors, such as exciton density, mobility, and diffusion length.[8,9] Trap states in organic semiconductors usually appear as charged traps, recombination centers, or a combination of both. Charged traps can impede carrier transport and hinder exciton dissociation in organic photodetector (OPD).[10] Additionally, Fermi level pinning may occur due to charged traps, leading to a reduction in the built-in electric field.[11] Therefore, it is crucial to gain a deeper understanding of trap states in organic semiconductors.

Currently, the commonly used methods for investigating density of state (DOS) distributions of OPD can be classified into three categories: (1) capacitance measurements,[9,12–14] (2) thermally stimulated current measurements,[15,16] and (3) conductance measurements.[17,18] Among these methods, trap state detection based on capacitance measurements is widely used. Capacitance measurement methods mainly include capacitance–voltage (CV) and capacitance–frequency (CF). Point-by-point CV can detect the trap state concentration at different positions in the depletion layer,[19] while forward bias CV (FB-CV) can determine the total concentration of shallow and deep traps.[20] However, all of these CV methods cannot obtain the distribution of trap states in the energy band. CF spectroscopy can investigate the energy level distribution of trap states,[14] but it can only detect shallow traps near the HOMO energy band. Although it is possible to measure the trap of deeper energy levels by lowering the frequency, the lower the frequency, the more noise it is, which makes it impossible to obtain reliable data. Even with the use of thick-film devices to reduce noise effects, only traps within 0.76 eV above the HOMO energy level can be detected under ultra-low-frequency condition, that is, 10 mHz.[19] It is well known that deep-level traps possess stronger capture capabilities than shallow traps[21] and can significantly impact device performance. However, recent methods are inadequate for characterizing deeper traps. In this Letter, a deep-level capacitance voltage (DLCV) method is proposed to characterize trap states in organic photodiode.

Figure 1 shows the band diagram of an OPD device at different bias voltages. As shown in Fig. 1(a), when the device is at a zero bias or small reverse bias voltage, only shallow traps are filled below the Fermi level. As shown in Fig. 1(b), the Fermi level rises with the increase in the reverse bias voltage, then the deeper traps will be also filled with electrons. Therefore, it is possible to obtain the deep trap distribution

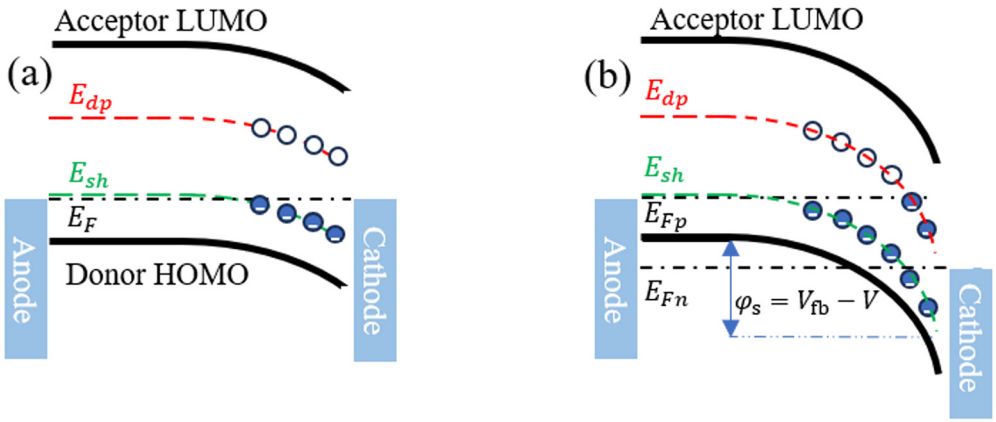

FIG. 1. (a) Energy band diagram at equilibrium (V= 0 and $E_F = E_{Fp} = E_{Fn}$). (b) Energy band diagram at reverse bias(V < 0).

information through the variation of capacitance with voltage. This situation is similar to the depletion state of the MOS device.[22] According to Poisson's equation, we have

$$\frac{d^2\varphi}{dx^2} = -\frac{\rho}{\varepsilon} = \frac{q}{\varepsilon}(n_{free} + n_{trap} - p_{free} - p_{trap}), \tag{1}$$

where n_{trap} and p_{trap} are the concentration of electron trap and hole trap, respectively, n_{free} is the concentration of free electron in the active layer, p_{free} is the concentration of free hole in the active layer, ε is the dielectric constant of the semiconductor, and ρ is the space charge density in the device. The unit area charge Q can be obtained by integrating the thickness direction of the space charge region of the device,

$$Q = \int_0^{t_s} \rho(x)dx = \int_{\varphi_s}^{0} \rho(x) \Big/ \frac{d\varphi}{dx} d\varphi, \tag{2}$$

where t_s is the thickness of the depletion region and φ_s is the potential difference between the surface and the body of the active layer. The capacitance of the space charge region per unit area can be obtained by differentiating Q with respect to the surface potential φ_s,

$$C_s = -\frac{dQ}{d\varphi_s} = \rho(\varphi_s) \Big/ \frac{d\varphi}{dx}\Big|_{x=0}. \tag{3}$$

According to the relation $\frac{d^2\varphi}{dx^2} = \frac{1}{2}\frac{1}{d\varphi}\left(\frac{d\varphi}{dx}\right)^2$, the electric field F at a point in the space charge region can be expressed as

$$F(\varphi) = -\frac{d\varphi}{dx} = \left[2\int_0^{\varphi_s} -\frac{\rho(\varphi)}{\varepsilon} d\varphi\right]^{\frac{1}{2}}. \tag{4}$$

From formulas (3) and (4), the expression of capacitance C_s in the space charge region can be obtained as

$$C_s = -\rho(\varphi_s)F(\varphi_s)^{-1}. \tag{5}$$

Based on Gauss's theorem $Q = \varepsilon \frac{d\varphi}{dx}|_{\varphi=\varphi_s}$, we have[22]

$$\rho(\varphi_s) = -\frac{1}{\varepsilon} Q \frac{dQ}{d\varphi_s}. \tag{6}$$

From the relationship $V = V_{fb} - \varphi_s$, where V is the applied voltage and V_{fb} is the flatband voltage, we get

$$C_s = \frac{dQ}{dV} = \frac{dQ}{d(V_{fb} - \varphi_s)} = -\frac{dQ}{d\varphi_s}, \tag{7}$$

$$Q = \int_{V_{fb}}^{V} C_s(V')dV', \tag{8}$$

$$\rho(\varphi_s) = \frac{C_s(\mathrm{V}) \int_{\mathrm{V_{fb}}}^{\mathrm{V}} C_s(V')dV'}{\varepsilon}. \tag{9}$$

According to Eq. (1),

$$\rho(\varphi_s) = -q\,(n_{free} + n_{trap} - p_{free} - p_{trap}) \tag{10}$$

with

$$n_{trap} = \int_{E_{HOMO}}^{E_F + q\varphi_s} N_t(E)dE, \tag{11}$$

$$p_{trap} = \int_{E_F + q\varphi_s}^{E_{LUMO}} P_t(E)dE, \tag{12}$$

$$n_{free} = n_0 e^{\frac{\varphi_s}{V_t}}, \quad p_{free} = p_0 e^{\frac{-\varphi_s}{V_t}}, \tag{13}$$

where $V_t = kT/q$, $N_t(E)$ is the density of electron trap states' distribution and $P_t(E)$ is the density of hole trap states' distribution. The derivative of (9) is obtained as follows:

$$N_t(E_F + q\varphi_s) + P_t(E_F + q\varphi_s) = -\frac{1}{q}\left(\frac{d\rho(\varphi_s)}{qd\varphi_s} + \frac{p_0}{V_t} e^{\frac{-\varphi_s}{V_t}} + \frac{n_0}{V_t} e^{\frac{\varphi_s}{V_t}}\right). \tag{14}$$

After determining the trap type in the device through the above-mentioned formula, the unit-area capacitance of the device tested by CV is approximately equal to C_s within the range of reverse bias and small positive bias. Then, ρ can be obtained by using Eq. (9), and the concentration of electron or hole traps can be obtained by using Eq. (14).

We fabricated a photodetector based on P3HT:PCBM with an area of 0.16 cm^2 and measure its characteristic to validate the aforementioned theory, as it contains deep-level traps that are difficult to detect by the conventional CF method.[19,20] P3HT (J&K scientific) and

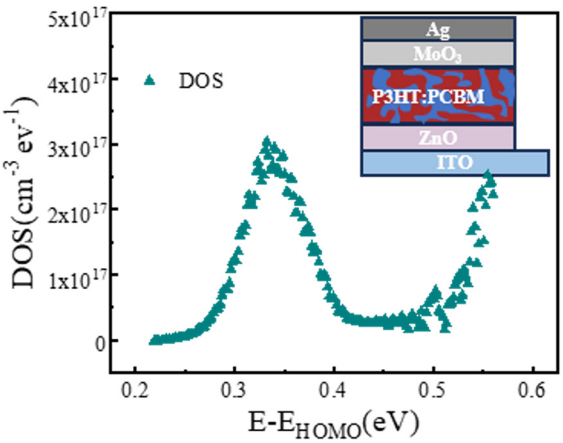

FIG. 2. DOS distribution extracted by the CF method (with the inset showing the structure of the devices).

PCBM (99.5%, J&K scientific) were mixed in a 1:1 (30 mg/ml) weight ratio in an ortho-dichlorobenzene solution, followed by stirring at 45 °C for 12 h inside a glovebox. The ZnO precursor solution[23] was spin-coated onto a ITO substrate at 3000 rpm for 20 s, followed by heating at 200 °C for 1 h to facilitate the formation of a dense ZnO film. Subsequently, the pre-prepared active layer solution was spin-coated onto the ZnO layer with parameters of 750 rpm and 20 s, followed by heating at 150 °C for 30 min. Under a vacuum pressure below 10^{-6} mbar, about 5 nm-thick MoO_3 was evaporated by thermal evaporation, followed by thermal evaporation of a 100 nm thick Ag electrode. The capacitance measurement was completed through the Keysight E5061B network analyzer.

The traditional CF method is used to measure the device in the frequency range of 10 Hz to 10 MHz to extract the trap state, and the test result is shown in Fig. 2 (the device structure is illustrated),

$$E_\omega = kTln\left(\frac{\omega_0}{\omega}\right) = E - E_{\mathrm{HOMO}}, \tag{15}$$

$$DOS(E_\omega) = -\frac{\omega V_{fb}}{qt_s kT}\frac{dC}{d\omega}, \tag{16}$$

where angular frequency ω is equal to $2\pi f$, ω_0 denotes an attempt-to-escape frequency, which usually lies within the order of 10^{12} s^{-1}, and E_ω represents the deepest detectable energy level. The trap distribution obtained by Eqs. (15) and (16), is shown in Fig. 2. Consistent with other works,[14,19] there is a shallow trap distribution peak at 0.34 eV above HOMO, while the deep trap about 0.55 eV above HOMO cannot be fully detected. The bandgap of most of the materials is much larger than 0.55 eV, which once again proves the necessity of extracting deep-level traps.

Before extracting the deep trap, we need to confirm whether electron traps or hole traps are in P3HT and PCBM. Therefore, single carrier devices with three different active layer materials P3HT, PCBM, and P3HT:PCBM were prepared for space-charge-limited-current (SCLC) measurement.[24] Comparing Figs. 3(a)–3(c), it can be seen that none of the hole-only devices have a slope greater than 2, which means that there are no hole traps in hole-only devices. Therefore, Eq. (14) can be simplified to Eq. (17). In addition, only electron-only devices containing P3HT have a slope of three, which means that electron traps are introduced by P3HT, consistent with previous studies.[17] Therefore, in the subsequent trap analysis, we mainly focused on P3HT,

$$N_t(E_F + q\varphi_s) = -\frac{1}{q}\left(\frac{d\rho(\varphi_s)}{qd\varphi_s} + \frac{p_{free}}{V_t}e^{\frac{-\varphi_s}{V_t}} + \frac{n_{free}}{V_t}e^{\frac{\varphi_s}{V_t}}\right). \tag{17}$$

To prevent the effects of low frequency noise and dielectric relaxation at high frequency, the CV measurement is performed at a frequency of 1 kHz.[20] Trap states obtained by the CF method use HOMO level as a reference, while our CV approach is based on the Fermi level E_F. To unify the two coordinates, corresponding tests are done to get Fermi levels and HOMO levels. As shown in Fig. 4(a), applying the Mott–Schottky relation[9]

$$\frac{1}{C^2} = \frac{2(V_{fb} - V)}{q\varepsilon N_t}, \tag{18}$$

V_{fb} can be obtained from the intercept in the $1/C^2$-V plot. Then, using $V_{fb} = (E_F - \varphi_M)/q$, the E_F of P3HT was determined to be −4.60 eV. From Figs. 4(b) and 4(c), the energy level of P3HT can be determined by cyclic voltammetry and ultraviolet–visible spectrophotometer. Using Ag/AgCl as the reference electrode, the HOMO energy level of

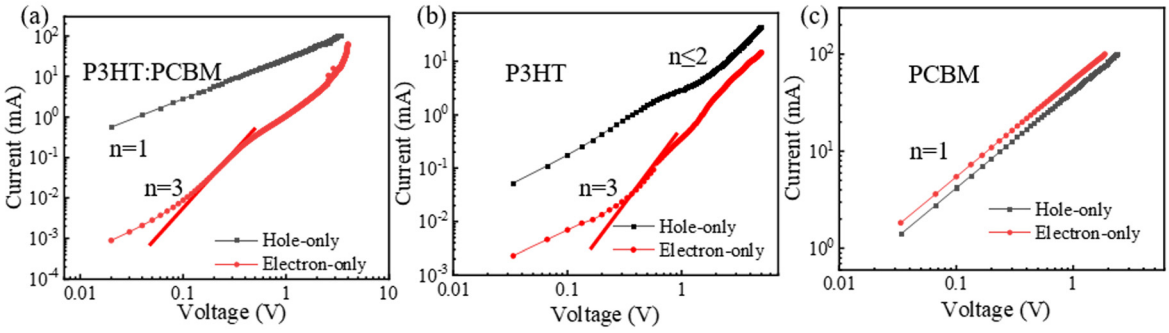

FIG. 3. SCLC measurement of single carrier devices with different active layer materials. (a) P3HT:PCBM bulk heterojunction mixed with 1:1 weight, while the slope of hole-only device is one, and the slope of electron-only device is three. (b) P3HT with electron-only devices slope n = 3. (c) PCBM has a slope of 1 for both electron-only and hole-only devices.

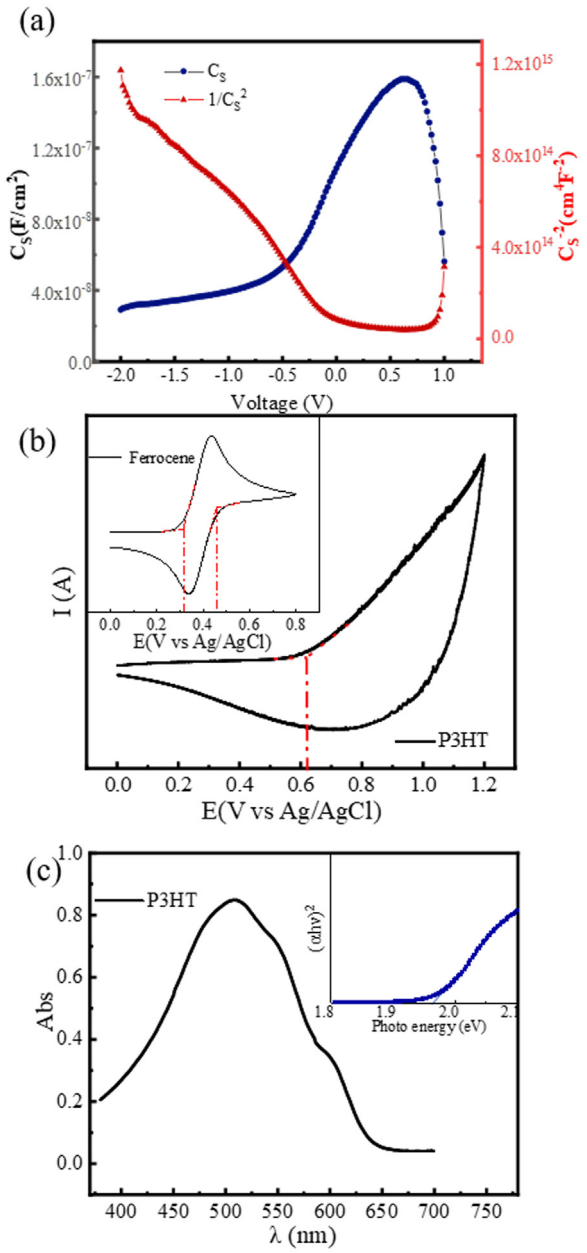

FIG. 4. (a) CV characteristics of OPD in 1 kHz. (b) Measurement of the oxidation energy level of P3HT, by cyclic voltammetry. The illustration shows the cyclic voltammetry measurement of ferrocene. (c) Ultraviolet–visible absorption spectroscopy (with inset showing the bandgap energy level fitting.

P3HT was measured to be −5.11 eV. The optical bandgap of P3HT can be obtained by UV-visible spectrum, and the LUMO energy level is further calculated to be −3.17 eV.[25]

According to CV data, $\rho(\varphi_s)$ can be extracted by Eq. (9), which allows extraction of $N_t(E)$ from Eq. 17. Figure 5 shows the DOS distribution extracted by DLCV and traditional CF, so that we can easily find the trap states extracted by the DLCV method, and the CF

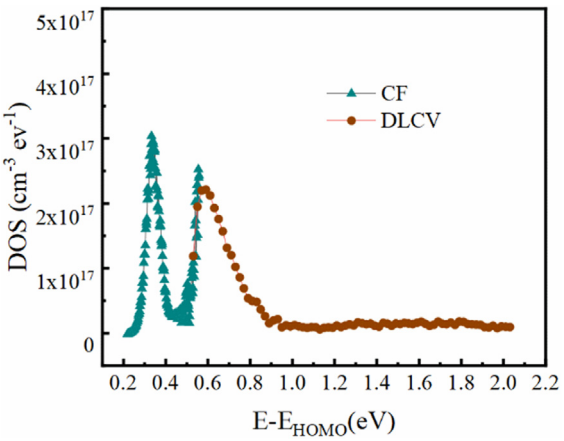

FIG. 5. DOS distribution extracted by the CF method and DLCV method; the DLCV method can detect deep traps and has good compatibility with the CF method.

methods can be well connected. The Gaussian distribution can be used to fit the two trap peaks of DOS, i.e.,

$$DOS(E) = \frac{N_t}{\sqrt{2\pi}\sigma}\exp\left[-\frac{(E-E_t)^2}{2\sigma^2}\right], \tag{19}$$

where N_t is the trap concentration, E_t is the trap energy level above HOMO, and σ is a disorder parameter that affects the broadening of Gaussian distribution.

From Table I, we can see that Peak1 has a higher concentration but a shallower location than Peak2. In addition, the DOS and trap energy levels of two peaks obtained by Gaussian fitting are similar to those obtained by the previous low-frequency CF method.[14,19] Moreover, the DLCV method yields a trap concentration of $8.06 \pm 0.33 \times 10^{16}\,\mathrm{cm}^{-3}$, while Mott–Schottky analysis yields a trap concentration of $8.31 \pm 0.54 \times 10^{16}\,\mathrm{cm}^{-3}$, demonstrating an agreement between these two methods and validating the reliability of the approach.

In this work, we propose a method of extracting deep trap distribution based on the CV measurement. The deep energy level traps are gradually filled with electrons with the increase in reverse bias, resulting in a change in charge. Therefore, the distribution of deep trap states can be derived from the relationship between capacitance and charge. To verify the trap type and location, the SCLC method is used. We find that this active layer only has electron traps, which are induced by P3HT. Subsequently, the Fermi level and the HOMO level of P3HT are obtained by the Mott–Schottky formula and cyclic voltammetry. After converting the DLCV method and the CF method to the same coordinate, it is easy to find that trap states extracted by the DLCV and the CF methods can be well connected. The Gaussian

TABLE I. DOS fitting parameters obtained from Eq. (19).

	N_t (cm^{-3})	E_t (eV)	σ (meV)
Peak 1	$6.01 \pm 0.55 \times 10^{16}$	0.340 ± 0.001	25.9 ± 1.6
Peak 2	$3.49 \pm 0.12 \times 10^{16}$	0.603 ± 0.004	103.0 ± 3.8

fitting results of them are close to those extracted by predecessors. Additionally, the total trap concentration in the bandgap obtained by the CF and the DLCV method is also consistent with the Mott–Schottky analysis. However, the DLCV method lacks the ability to accurately extract the distribution of trap states when both electron and hole traps are present in organic photodiode. Nevertheless, organic materials containing both traps are rare.[26] Therefore, the DLCV method may still be very valuable for characterizing the deep traps' distribution of OPD or OPV, which the CF method cannot do.

This work was supported in part by each of the following institutions: the MOST (Grant Nos. 2021YFB3600800 and 2022YFB3603103), the NSFC (Grant Nos. 62074059 and 22090024), the Fundamental Research Funds for the Central Universities (Grant No. 2023ZYGXZR002), the Natural Science Foundation of Guangdong Province (Grant Nos. 2021A1515011951 and 2022A1515011633), and the Science and Technology Program of Guangdong Province (Grant No. 2019B010934001).

AUTHOR DECLARATIONS

Conflict of Interest

The authors have no conflicts to disclose.

Author Contributions

Wencai Zuo: Conceptualization (lead); Data curation (lead); Formal analysis (lead); Investigation (lead); Methodology (lead); Writing – original draft (lead); Writing – review & editing (lead). **Sai Liu:** Investigation (equal); Supervision (equal); Writing – review & editing (equal). **Haoyang Li:** Conceptualization (equal); Methodology (equal); Supervision (equal); Writing – review & editing (equal). **Lianjie Zhang:** Funding acquisition (equal); Investigation (supporting). **Weijing Wu:** Conceptualization (equal); Funding acquisition (lead); Investigation (equal); Methodology (equal); Project administration (lead); Resources (lead); Supervision (equal); Writing – review & editing (equal). **Junwu Chen:** Investigation (supporting). **Junbiao Peng:** Funding acquisition (lead); Investigation (supporting); Resources (equal).

DATA AVAILABILITY

The data that support the findings of this study are available from the corresponding authors upon reasonable request.

REFERENCES

[1]H. Haixia, M. Xinyu, Q. Wei, G. Kun, H. Xiaotao, and Y. Hang, Appl. Phys. Lett. **120**, 023302 (2022).
[2]L. Zhang, F. Yang, W. Deng, X. Guo, Y. He, J. Zhou, H. Li, Y. Zhang, K. Zhou, C. Zhou, Y. Zou, J. Yang, X. Hu, W. Ma, and Y. Yuan, Appl. Phys. Lett. **122**, 263903 (2023).
[3]Y. Song, Z. Zhong, P. He, G. Yu, Q. Xue, L. Lan, and F. Huang, Adv. Mater. **34**, e2201827 (2022).
[4]S. Deng, L. Zhang, J. Zheng, J. Li, S. Lei, Z. Wu, D. Yang, D. Ma, and J. Chen, Adv. Opt. Mater. **10**, 2200371 (2022).
[5]A. Ghorai, S. S. Behera, S. Purohit, and K. S. Narayan, Appl. Phys. Lett. **122**, 203301 (2023).
[6]M. Xu, H. Zhou, L. Chen, Y. Meng, W. Lv, L. Zhang, S. Liu, and W. Xie, Appl. Phys. Lett. **122**, 261107 (2023).
[7]W. Shin, J. Shin, J.-H. Lee, H. Yoo, and S.-T. Lee, Appl. Phys. Lett. **122**, 263506 (2023).
[8]T.-Y. Chu and O.-K. Song, J. Appl. Phys. **104**, 023711 (2008).
[9]J. V. Li, A. M. Nardes, Z. Liang, S. E. Shaheen, B. A. Gregg, and D. H. Levi, Org. Electron. **12**, 1879 (2011).
[10]C. R. McNeill, I. Hwang, and N. C. Greenham, J. Appl. Phys. **106**, 024507 (2009).
[11]G. Garcia-Belmonte, P. P. Boix, J. Bisquert, M. Sessolo, and H. J. Bolink, Sol. Energy Mater. Sol. Cells **94**, 366 (2010).
[12]A. R. Frederickson and A. S. Karakashian, J. Appl. Phys. **77**, 1627 (1995).
[13]O. Gunawan, T. Gokmen, C. W. Warren, J. D. Cohen, T. K. Todorov, D. A. R. Barkhouse, S. Bag, J. Tang, B. Shin, and D. B. Mitzi, Appl. Phys. Lett. **100**, 253905 (2012).
[14]P. P. Boix, G. Garcia-Belmonte, U. Munecas, M. Neophytou, C. Waldauf, and R. Pacios, Appl. Phys. Lett. **95**, 233302 (2009).
[15]J. Schafferhans, C. Deibel, and V. Dyakonov, Adv. Energy Mater. **1**, 655 (2011).
[16]J. Schafferhans, A. Baumann, C. Deibel, and V. Dyakonov, Appl. Phys. Lett. **93**, 093303 (2008).
[17]H. T. Nicolai, M. Kuik, G. A. H. Wetzelaer, B. de Boer, C. Campbell, C. Risko, J. L. Bredas, and P. W. M. Blom, Nat. Mater. **11**, 882 (2012).
[18]V. I. Arkhipov, P. Heremans, E. V. Emelianova, and G. J. Adriaenssens, Appl. Phys. Lett. **79**, 4154 (2001).
[19]J. A. Carr and S. Chaudhary, J. Appl. Phys. **114**, 064509 (2013).
[20]B. Ray, A. G. Baradwaj, B. W. Boudouris, and M. A. Alam, J. Phys. Chem. C **118**, 17461 (2014).
[21]L. G. Kaake, P. F. Barbara, and X. Y. Zhu, J. Phys. Chem. Lett. **1**, 628 (2010).
[22]W.-J. Wu, C.-L. Chen, X. Hu, X.-H. Xia, L. Zhou, M. Xu, L. Wang, and J.-B. Peng, J. Disp. Technol. **12**, 888 (2016).
[23]Y. Sun, J. H. Seo, C. J. Takacs, J. Seifter, and A. J. Heeger, Adv. Mater. **23**, 1679 (2011).
[24]J. Zhou, D. He, Y. Li, F. Huang, J. Zhang, C. Zhang, Y. Yuan, Y. Lin, C. Wang, and F. Zhao, Adv. Mater. **35**, 2207336 (2023).
[25]U. K. Verma, S. Kumar, and Y. N. Mohapatra, Sol. Energy Mater. Sol. Cells **172**, 25 (2017).
[26]N. B. Kotadiya, A. Mondal, P. W. M. Blom, D. Andrienko, and G.-J. A. H. Wetzelaer, Nat. Mater. **18**, 1182 (2019).